



Optimization of the 30 gross tonnage fiberglass fishing boat hull to obtain optimal main motor power.

Amir Marasabessy¹, Damora Rhakasywi^{2,*}, Sargi Ginting³

ARTICLE INFO

Article history:

Received 30 Jan 2023;
in revised from 30 Jan 2023;
accepted 18 Feb 2023.

Keywords:

Fishing Boat, Optimum Power,
Optimum main motor power,
Fiberglass, Gross Tonnages.

ABSTRACT

The design and production of 30 gross tonnages (GT) fiberglass fishing boats do not yet have technical and economic accuracy. The purpose of this study is to design a 30 GT fiberglass fishing boat hull model to find the minimum speed of the ship, the optimum power of the main motor of the ship and the appropriate gross tonnage of the ship. The method used in this planning is optimization of preliminary design and optimization of design approach to obtain optimal ship size and main motor power. Based on the results of ship planning, the product design is obtained in the form of drawings of lines plan and general arrangement with the main size of the ship (Loa) 20.50 meters, ship width (B) = 4.27 meters, deck height = 18.75 meters and draft = 1.20 meters. Optimum main motor power (BHP) = 150 Hp, with service speed (Vs) = 10.5 knots. The conclusion meets the appropriate gross tonnage of 30 GT based on the general arrangement planning which has good ship stability with a rolling period of 80.58 seconds.

© SEECMAR | All rights reserved

1. Introduction.

The materials used for the production of fishing boats using fiberglass are superior because these materials are easy to obtain in the market and the production costs are very competitive and do not require a large investment with a fast production process (Marasabessy and Siagian, 2016), this is when compared to steel, both production and maintenance costs are very expensive and require a large investment for the production process (Ma'ruf, 2011), (Marcell, Supomo and Arif, 2021), (Viljoen et al., 2022), (Yang, Peng and Wang, 2018).

Research that has been done previously is the design of fishing boats with 5 GT and 10 GT but is still in the preliminary

design stage (Marasabessy et al., 2019), (Sudjasta and Djaya, 2015). Strength of the hull made of fiberglass with different thickness variations (Wolok et al., 2017), (A.J.Sobey, J.I.R.Blake and R.A.Shenoi, 2013). Previous research conducted a review of the extent to which the application of classification rules in the production process of building 3 GT fishing boat by testing the tensile strength and bending strength of the laminated specimens of the 3 GT fiber reinforced plastic (FRP) fishing boat (Marzuki, 2017). Another study used Chopped Strand Mat (CSM) and Woven Roving Mat (WRM) which were combined to produce a laminated structure of Glass Fiber Reinforced Polymer (GFRP) on small vessels such as fishing vessels, hull plates were verified quantitatively through experiments and statistical analysis (Oh et al., 2022).

Non-contact underwater explosion (UNDEX) can cause very large deformations in composite structures associated with severe nonlinear phenomena. In previous studies composite materials were characterized by experimental modal analysis as well as a comprehensive series of shock tests, the results of which were compared with a numerical model, in which the composite specimen is supported on a special confining structure designed to create large deflections and provide reproducible re-

¹Faculty of Engineering, Naval Engineering, Universitas Pembangunan Nasional Veteran Jakarta, Jl. Limo Raya No.80, Limo, Kec. Limo, Kota Depok, Jawa Barat 16514. Indonesia.

²Faculty of Engineering, Mechanical Engineering, Universitas Pembangunan Nasional Veteran Jakarta, Jl. Limo Raya No.80, Limo, Kec. Limo, Kota Depok, Jawa Barat 16514. Indonesia.

³Faculty of Engineering, Naval Engineering, Universitas Pembangunan Nasional Veteran Jakarta, Jl. Limo Raya No.80, Limo, Kec. Limo, Kota Depok, Jawa Barat 16514. Indonesia.

*Corresponding author: Damora Rhakasywi Tel. 021-7656904/75817114
E-mail: rhakasywi@upnvj.ac.id.

sults (Mannacio et al., 2022).

In other studies the suitability of S-Glass/carbon fiber reinforced polymer composites for submarine hulls subjected to hydrostatic pressure, metallic materials has raised concerns due to their decomposition and low resistance to salinity. In this study, the mechanical properties of S-Glass/carbon fiber reinforced polymer composites were investigated experimentally with higher specific strength and composite stiffness compared to many metal materials. The nonlinear impact at speed (3 - 21) m/s as well as kinetic energy, peak acceleration and internal energy on the submarine explained at a certain depth with travel (1750 - 3500)m is recommended, more specifically the submarine accident safety factor is found to be within limits when the submarine is at a depth of 1750 m (Natarajan et al., 2022). Other studies have used composite materials, especially glass fiber reinforced polymer composites (GFRP). Previous studies have established that seawater aging has a detrimental effect on the physical and mechanical properties of GFRPs, the current study examining the effect of seawater aging at a macroscopic level. The results show a higher failure rate in the seawater treated composites compared to the untreated composites (Bhat, Mohan and Sharma, 2022). Other studies using fiberglass-reinforced composite materials are commonly used in engineering structures that are subjected to dynamic loading, such as wind turbine blades, automobiles, and airplanes. The study utilized piezoresistive laser induced graphene (LIG) integrated into fiberglass-reinforced composites for fatigue damage monitoring and life prediction (Groo et al., 2021).

The previous study discussed the damage to dome and graffiti materials that were affected by the type of hard degradation, very different from those affecting historic building materials, which jeopardized their preservation conditions. The study investigated whether a conservative restoration methodological approach could be applied to this structure, which is an example of contemporary architecture. The degradation affecting the dome and graffiti was then investigated, as well as the fiberglass samples (Pizzigatti and Franzoni, 2021). Research on manufacturing technology for advanced composite materials, the use of composites for engineering applications has increased significantly. The purpose of this research is to study the response of an ideal subsystem made of composite material and then study the vibration response theoretically using the Statistical Energy Analysis (SEA) method. The results of this study obtained the modal density of rectangular composite plates made of fiberglass experimentally and theoretically (Borgaonkar, Mandale and Potdar, 2018).

The next study examined the mechanical and physical properties of hybrid composites made by adding plain woven copper strip mesh between fiberglass layers in Glass-Fiber Reinforced Plastics (GFRP) composites before curing. The results showed that there was an increase in the tensile strength of 16.357% in the hybrid composite compared to the GFRP composite, the flexural strength of the hybrid composite increased by 29.019%, where the impact energy of the hybrid composite increased by 55.55%, the density of the hybrid composite increased by 57.208% and the hardness of the hybrid composite increased by 13.846% (Chopra et al., 2022). Other research on

natural rubber fiber (NR) products is increasing because natural rubber can be obtained from nature and can be produced into sustainable products, widely used in applications such as tires, cables, latex products, medical devices, and sports components. In this study, the use of electrospinning technique to produce fiber has been carried out because this technique has proven to be a simple and effective technique for fiber production. This study aims to study the morphology, diameter, and functional groups of natural rubber fibers and the differences in lignin loading on the fibers produced by electrospinning technique (Ngamkham et al., 2021). Subsequent research on fibers investigated the thermal and mechanical neutron attenuation properties of reinforced concrete using low-dose gamma irradiated polyethylene terephthalate (PETE) fibers. The results showed that fiber reinforced concrete (FRC) which had 25 denier fibers provided higher compressive strength, flexural strength, and toughness than FRC with 1.3 denier fibers (Khemngern et al., 2020).

Future research will focus on natural fibers which are very useful with strong mechanical properties. In this study, fiberglass reinforced with unsaturated polyester composites were tested for water absorption. The water absorption test was carried out by immersing the test object into three different environmental conditions, namely sea water, distilled water and rain water. Results In general, the mechanical properties of natural fibers deteriorate after moisture enters the composite. Strain to failure increased from the first day to the 4th week, the humidity received was evidence found on scanning electron microscopy (SEM) micrographs that had an effect on decreasing the tensile modulus (Ghani et al., 2012).

Thermal oxidation of the unidirectional carbon fiber/glass fiber hybrid composite was investigated to determine the oxidation kinetics and degradation mechanism. The resultant tensile strength remained essentially unchanged by thermal oxidation after 52 weeks of exposure. Inspection of thermally aged sealed rods shows no cracks after long term exposure (E.Barjasteh et al., 2009). Another study showed the results of experimental studies on laminated Kevlar/fiberglass composites subjected to impact loading at various temperatures. Effect of temperature on maximum energy, elastic energy, maximum deflection, maximum impact force, and compression. The temperature under consideration is in the range of 50 to 120 °C. The results show that the impact performance of this composite is influenced by the temperature range used (Salehi-Khojin et al., 2006).

Other studies in recent years have increasingly recognized the importance of reducing ship fuel consumption on sea routes to reduce greenhouse gas emissions from shipping. From a ship design point of view, it is very important to establish reliable predictive methods for ship resistance and propulsion. There are three solutions for the prediction of ship resistance as follows analytical method, in-tank model test and Computational Fluid Dynamics (CFD). This study aims to simulate ship resistance using the CFD simulation method which was carried out using the ANSYS-CFX software package. The results showed that the ship's resistance was calculated at various ship speeds and Froude numbers. The predicted results for the resistance components at various Froude numbers are compared with the

resistance results calculated using the Holtrop method. It can be seen that the simulation results are quite in agreement with the results calculated from the Holtrop method, and the ANSYS-CFX code can predict ship resistance. (Elkafas, Elgohary and Zeid, 2019),(Poundra et al., 2017),(Orych, Werner and Larsson, 2021). To reduce and minimize the discrepancy of a design against the owner’s requirement at the design stage, it is necessary to conduct a study in preliminary ship design with optimization methods to determine the main size of the ship and the optimal hull form (Hadi and Zain, 2011), (Faculty, 2022).

The flow that occurs in waves forms along the hull of the ship and the expansion flow behind the hull can absorb energy from the ship. Ship resistance and the behavior of its components are very important in estimating ship propulsion, which can positively affect fuel consumption (Sulistyawati, Yanuar and Pamitran, 2020).

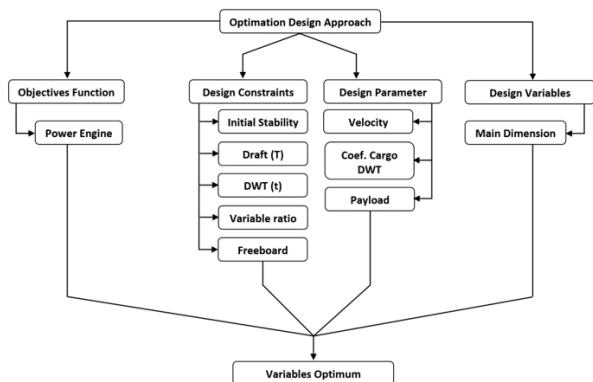
Evaluation of the hydrodynamic efficiency of the ship resulting from energy-efficient and concentrated cost functions. Optimization method with hull geometry representation is one of the most appropriate initial design steps to evaluate hydrodynamic performance (Sulistyawati and Suranto, 2009).

The specific objective of this research is to plan a 30 GT fiberglass fishing boat hull model to be able to help coastal fishermen. This research was carried out by developing the technology for making a 30 GT fishing boat hull model in 3D and determining the optimal main size of the ship so as to get the right gross tonnage, precision, appropriate ship speed and good ship stability, equipped with tools to call fish using sound waves.

2. Optimization Design Approach.

The design optimization method in this research aims to determine the main size of the ship based on the design limits of the registered comparison ship. The optimization method is used to determine the optimum main size of the ship and the power requirements of the propulsion motor at the basic design stage (Manual, 2022). The optimization design approach is chosen as an alternative that can produce the optimum value from certain criteria by determining the parameters that must be met and the constraints set as shown in the diagram (Okumoto et al., 2009) in Fig. 1.

Figure 1: Design Approach optimization flow.

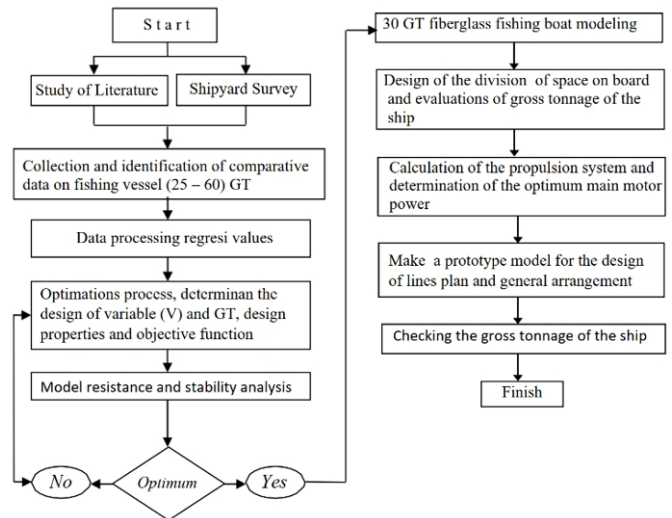


Source: Authors.

3. Research Methods.

In planning the hull of a fishing boat made of fiberglass to obtain optimal main motor power, the research team carried out the design process and made a modeling of the hull. The overall research stages can be seen in the flow chart shown in Fig. 2.

Figure 2: Diagram of research stages.



Source: Authors.

- The optimization process carried out on the design of the 30 GT fiberglass fishing boat hull model is using Excel Solver. Optimization of Microsoft Excel add-in Solver by specifying Design variables: L, B, T, H, Cb. Parameters: speed (owner requirement) and gross tonnage. Design constraints on the requirements that apply to fishing vessels. Design properties include calculations: Displacement LWT, DWT, Trim, Initial Stability and Resistance. Objective function: minimizing the main engine power, maximizing the stability and maximizing speed.
- Analysis of resistance and stability using Maxsurf, Hullspeed and Hydromax software. Hullspeed is used to test the resistance and power of the model and at the same time to determine the maximum speed and efficiency. Meanwhile, for the analysis of the stability of the ship model, Hydromax Pro was used to determine the characteristics of the forces acting on the submerged part of the model.
- Correction of the difference between numerical and experimental calculations is a maximum of 0.5%, where the smaller the value of the percentage difference, the better the level of validation. If the comparison between numerical calculations and experiments exceeds the maximum percentage deviation, the numerical calculation process must be evaluated again.
- Determination of the most optimal model can be seen from the results of the analysis of resistance. The result of the smallest resistance will then be analyzed for its stability. If it does not get the appropriate stability results, then the next small resistance value is chosen again until the stability that meets the requirements is obtained.

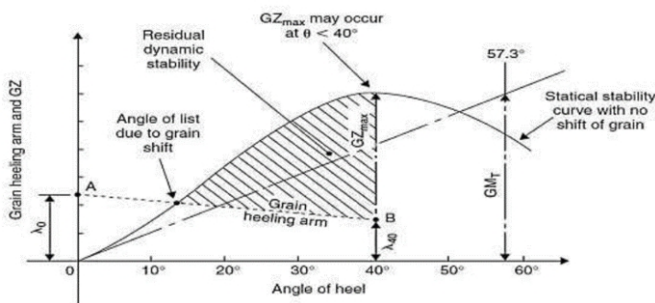
The steps for the optimization process using the Microsoft Excel add-in Solver include:

- a. Design variables: The initial main measure of the design variable according to the polynomial regression process: whole length (Loa) = 19.06 m, ship width (B) = 4.72 m, deck height (H) = 2.13 m, laden height (T) = 1.28 m, coefficient block (Cb) = 0.55
- b. Design parameters: gross tonnage = 30 RT, ship speed (V_k) = 10 knot.
- c. Design constraints include: variable from the main size of the ship: laden height $0.7 \leq T \leq 1.60$ m, coefficient block $0.5 \leq C_b \leq 0.6$, main size design variable ratio: $2.90 \leq L/B \leq 5.25$, $7.20 \leq L/H \leq 13.40$, $12.00 \leq L/T \leq 24.40$, $2.80 \leq B/T \leq 4.00$, $1.65 \leq B/H \leq 2.75$.

4.2. Stability Analysis Using Hydromax Software.

The main parameter in determining the durability of the ship is to have good stability (Jiao, Ren and Sun, 2016). Ship stability is determined by several factors such as the shape of the hull, weight and the location of the center of gravity when the ship is operating. The condition of the ship operating always changes in weight and the location of the center of gravity. Assessment of stability is seen from the shape of the static stability curve of the GZ curve, where GZ is the size of the ship’s return arm under certain shaky conditions. Stability calculations are carried out to analyze the safety aspects of the designed ship. The stability criteria are shown in Fig. 8, based on the general intact stability criteria for all ships (Organization, 1993).

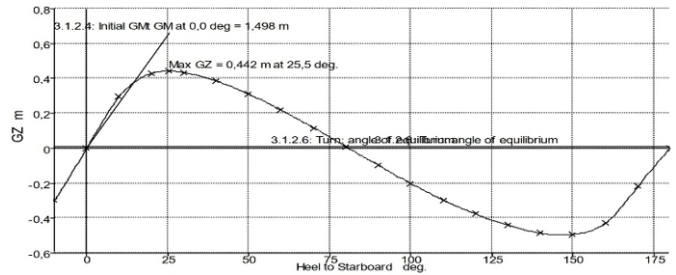
Figure 8: Stability according to IMO requirements (Organization, 1993).



Source: Authors.

Fig. 8. Shows that the area of the curve under the static arm curve (GZ) should not be less than 0.055 m radians or 3.151 m. degree up to 30° angle of sway. The area under the return arm curve (GZ curve) to an angle of 40° is not less than 0.090 m. rad or 5.157 m. degree. The area under the curve of the static arm (GZ) between the sway angles of 30° and 40° shall not be less than 0.03 m radians or 1.719 m. degree. Static Arm (GZ) at a swing angle of more than 30° shall not be less than 0.20 m. Maximum return arm occurs at a swing of more than 30° but not less than 25°.

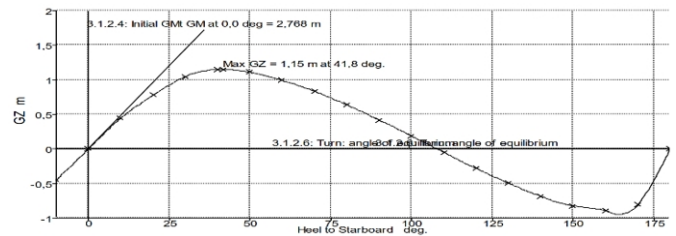
Figure 9: Stability at 100% load transfer.



Source: Authors.

Fig. 9. Explains the condition of 100% load transfer stability meeting the requirements required by International Maritime Organization (IMO), namely the area under the stability curve between the wobble angles of 0° to 30° is 9.714m.deg, which is more than the minimum required of 3.151m.deg. The criteria for the maximum enforcement arm (GZ) angle are also met where the requirements that must be met are at least 25°, the results obtained are the GZ angle of 25.50°.

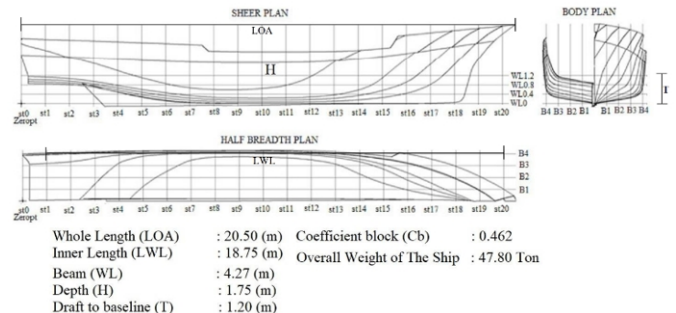
Figure 10: Stability at empty load.



Source: Authors.

Fig.10. Explains that under the condition of an empty load, the stability meets those required by IMO, namely the area under the stability curve between the wobble angles of 0° to 30° is 17.659m.deg, which is greater than the minimum required at 3.151m.deg. For the maximum GZ angle criteria are also met where the requirements that must be met are at least 25°, the results obtained are 41.80° GZ angles.

Figure 11: Ship line plan.

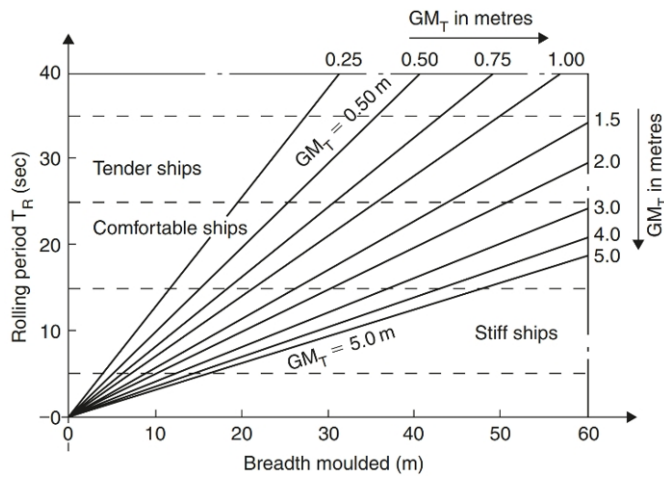


Source: Authors.

Fig. 11. Shows a ship line plan drawn using Maxsurf software with a LOA value of 20.50 m, length 18.75 m, beam is

4.27 m, depth is 1.75 m, draft to baseline is 1.20 m and the overall weight of the ship is 47.80 tons.

Figure 12: Rolling period (Barrass and Derrett, 2006).



Source: Authors.

Fig. 12. Shows the resulting rolling period based on the GM_T variable 5.0 m and the B width 60 m. From the graph it can be seen: (a) The roll time period does not depend on the actual amplitude of the coil as long as the angle is small, (b) The roll time period varies directly as K, the radius of gyration. If the radius of gyration is increased, the time period is also increased. K can be increased by moving the load away from the axis of oscillation. The average K value is about $0.35 \times Br.Mld$, (c) The overturning time period is inversely proportional to the square root of the initial metacentric height. If the ship with a large GM will have a short period and a ship with a small GM will have a long period, (d) The overturning period will change as the load is loaded, unloaded or shifted in the vessel, as this usually affects both the radius of gyration and the initial metacentric height (Barrass and Derrett, 2006). The result of the calculation of the sway period is 20.58s. The ship’s shaky period is between 30-35 (s) it can be said that the ship has a stability that is not rigid and causes discomfort in the motion of the ship and passengers. While the period of the ship is below 8 (s) it can be said that the ship has a rigid stability (stiff) which also causes discomfort in the movement of the ship and passengers because the ship is rocking too fast. For ships that have a good shaking period ranging from 20-25 (s) (Barrass and Derrett, 2006). So it can be said that this fishing boat has good stability with a shaking period of 20.58 s.

4.3. Gross Tonnage (GT) Check.

Gross Tonnage (GT) of the ship is the total volume of space below and above the strength deck (main deck in accordance with the General Arrangement drawing), which is then multiplied by a gross tonnage coefficient of 0.353, in Fig. 11. Determination of Gross Tonnage of fiberglass fishing boats, as shown in table 1.

Table 1: Determination of Gross Tonnage of Ships.

No.	Room	Size (length x width x height), m	Volume (m ³)
A Beneath the deck of strength			
1	bow niche	(1.84 x 1.08 x 0.70) x 75%	1.04
2	rigging	(2.05 x 1.19 x 1.44) x 80%	2.81
3	net	(1.23 x 3.20 x 1.34)	5.28
2	palka 1	(1.23 x 3.21 x 1.34)	5.29
3	palka 2	(2.05 x 3.56 x 1.34)	9.78
4	palka 3	(2.46 x 3.79 x 1.34)	12.49
5	engine room	(5.84 x 3.91 x 1.23) x 75%	21.05
6	stern niche	(1.53 x 3.08 x 1.03) x 75%	3.64
B Above the deck of strength			
1	platform	(5,23 x 3,08 x 1,85) x 80%	24.30
Total room volume			85.68

Source: Authors.

Conclusions.

The results of the calculation of the 30 GT fiberglass fishing boat design at the preliminary design stage, can be concluded as follows:

- The basic size of the ship (Loa) is 20.50 meters, the width of the ship (B) = 4.27 meters, the deck height = 18.75 meters and the draft = 1.20 meters. Optimum main motor power (BHP) = 150 Hp, with ship speed during normal voyage = 10.5 knots.
- Gross tonnage (GT) of the boat reaches 30 GT based on the general arrangement.
- Under the condition of an empty load, the stability meets those required by International Maritime Organization (IMO), namely the area under the stability curve between the wobble angles of 0° to 30° is $17.65948m.deg$, which is greater than the minimum required of $3.151m.deg$. For the maximum (GZ) angle criteria are also met where the requirements that must be met are at least 25° , the results obtained are 41.80° enforcement arm (GZ) angles.
- The designed fishing vessel has a fairly good stability with a shaking period value of 20.58s, because for a vessel that has a good shaking period it ranges from 20-25 (s).
- The results of the analysis of motion at forward speed with a wave direction of 180° are very good. For translational motion, it is known that the highest amplitude occurs at Response Amplitude Operator (RAO) surge motion (X) of 3.55

($^{\circ}/m$) at a frequency (ω) of 0.005 Hz, and rotational motion it is known that the highest amplitude occurs at RAO pitch motion (RY) of $8.63E+07(^{\circ}/m)$ at a frequency (ω) of 0.187 Hz.

Acknowledgements.

This work was supported within the LPPM (Lembaga Penelitian dan Pengabdian Kepada Masyarakat) – Universitas Pembangunan Nasional Veteran Jakarta (Project number: 268/UN.61.0/HK.07/LIT.RISCOP/2022).

References.

- A.J.Sobey, J.I.R.Blake and R.A.Shenoi (2013) ‘Optimisation of composite boat hulls using first principles and design rules’, *Ocean Engineering*, 65(0), pp. 62–70. doi: 10.1016/j.oceaneng.2013.03.001.
- Barrass, C. B. and Derrett, D. R. (2006) ‘Ship Stability for Masters and Mates’, in Barrass, C. B. (ed.). *Sciencedirect - Elsevier Ltd*. Available at: <https://www.sciencedirect.com/book/9780750667845/ship-stability-for-masters-and-mates>.
- Bhat, R., Mohan, N. and Sharma, S. (2022) ‘Effect of Sea-water Immersion on the Drill Induced Delamination Failure in Glass Fiber Reinforced Polymer Composites - Experimental And Statistical Analysis’, *Engineering Failure Analysis*, pp. 1–15. doi: 10.1016/j.engfailanal.2022.106803.
- Borgaonkar, A. ., Mandale, M. . and Potdar, S. . (2018) ‘Effect of Changes in Fiber Orientations on Modal Density of Fiberglass Composite Plates’, in *Materials Today: Proceedings*. Elsevier Ltd, pp. 5783–5791. doi: 10.1016/j.matpr.2017.12.175.
- Chopra, R. et al. (2022) ‘Experimental study on mechanical properties of E-Glass fiber reinforced with epoxy resin composite and compare its properties with hybrid composite’, *Materials Today: Proceedings journal*, 63, pp. 417–421. doi: 10.1016/j.matpr.2022.03.435.
- E. Barjasteh et al. (2009) ‘Thermal aging of fiberglass/carbon-fiber hybrid composites’, *Composites Part A: Applied Science and Manufacturing*, 40(12), pp. 2038–2045. Available at: <https://www.sciencedirect.com/science/article/abs/pii/S1359835X09002905>.
- Elkafas, A. G., Elgohary, M. M. and Zeid, A. E. (2019) ‘Numerical study on the hydrodynamic drag force of a container ship model’, *Alexandria Engineering Journal*, 58(3), pp. 849–859. doi: 10.1016/j.aej.2019.07.004.
- Faculty, A. H. (2022) ‘Multi-objective optimization method of trimaran hull form for resistance reduction and propeller intake flow improvement’, *Ocean Engineering*, 244(December 2021), p. 110352. doi: 10.1016/j.oceaneng.2021.110352.
- Ghani, M. A. . et al. (2012) ‘Mechanical Properties of Kenaf/Fiberglass Polyester Hybrid Composite’, in *Procedia Engineering*, pp. 1654–1659. doi: 10.1016/j.proeng.2012.07.364.
- Groo, L. et al. (2021) ‘Fatigue damage tracking and life prediction of fiberglass composites using a laser induced graphene interlayer’, *Composites Part B: Engineering*, 218(April), pp. 1–8. doi: 10.1016/j.compositesb.2021.108935.
- Hadi, E. S. and Zain, A. (2011) ‘Preliminary study of general cargo ship hull form design for shipping from Jakarta to Makassar using a deterministic approach’, *Kapal*, 8(1), pp. 41–52. doi: 10.12777/kpl.8.1.41-52.
- Jiao, J., Ren, H. and Sun, S. (2016) ‘Assessment of surface ship environment adaptability in seaways: A fuzzy comprehensive evaluation method’, *International Journal of Naval Architecture and Ocean Engineering*, 8(4), pp. 344–359. doi: 10.1016/j.ijnaoe.2016.05.002.
- Khemngern, S. et al. (2020) ‘Mechanical and Thermal Neutron Attenuation Properties of Concrete Reinforced with Low-Dose Gamma Irradiated PETE Fibers and Sodium Borate’, *Engineering Journal*, 24(3), pp. 1–10. doi: 10.4186/ej.2020.24.3.1.
- Ma’ruf, B. (2011) ‘A Study on Standardization of Fiberglass Ship’s Hull Lamination Construction’, *Jurnal Standardisasi*, 13(1), pp. 16–25.
- Mannacio, F. et al. (2022) ‘Characterization of underwater shock transient effects on naval E-glass biaxial fiberglass laminates: An experimental and numerical method’, *Applied Ocean Research journal*, 128(April), pp. 1–17. doi: 10.1016/j.apor.2022.103356.
- Manual, A. (2022) ‘Maxsurf’, in Clarke, S. (ed.). *Horsebridge Hill, Newport, Isle of Wight, England: Maxsurf*. Marasabessy, A. et al. (2019) ‘Initial Design of a Fishing Boat Made of Fiberglass With a Capacity of 30 GT’, *Jurnal Ilmiah GIGA*, 22(2), pp. 68–74. doi: 10.47313/jig.v22i2.769.
- Marasabessy, A. and Siagian, S. (2016) ‘Fiberglass hull zone crack analysis’, in *National Seminar on Science & Technology Applications (SNAST)*, pp. 151–158.
- Marcell, M. R. R., Supomo, H. and Arif, M. S. (2021) ‘Technical And Economic Analysis Comparison Of The Corrosion Rate Of Galvanized And Aluminum Materials To Predict The Life And Cost Of Hull Repairs’, *ITS Engineering Journal*, 10(2). doi: 10.12962/j23373539.v10i2.80372.
- Marzuki, I. (2017) *Study of Standardization of Laminated Structure of Fiberglass Fishing Boat Hull 3 GT*. Institut Teknologi Sepuluh Nopember Surabaya.
- Natarajan, E. et al. (2022) ‘Experimental and numerical analysis on suitability of S-Glass-Carbon fiber reinforced polymer composites for submarine hull’, *Defence Technology*, pp. 1–11. doi: 10.1016/j.dt.2022.06.003.
- Ngamkham, R. et al. (2021) ‘Production of Composite Fibers from Natural Rubber and Lignin’, *Engineering Journal*, 25(4), pp. 79–85. doi: 10.4186/ej.2021.25.4.79.
- Oh, D. et al. (2022) ‘Effects of fabric combinations on the quality of glass fiber reinforced polymer hull structures’, *International Journal of Naval Architecture and Ocean Engineering*, 14, pp. 1–10. doi: 10.1016/j.ijnaoe.2022.100462.
- Okumoto, Y. et al. (2009) *Design of ship hull structures: A practical guide for engineers*, *Design of Ship Hull Structures: A Practical Guide for Engineers*. doi: 10.1007/978-3-540-88445-3.
- Organization, I. M. (1993) ‘Code on intact stability for all type of ships covered by IMO instruments’, in *Resolution A.749 (18)*. 11th edn. *International Maritime Organization*, pp. 255–331. Available at: <https://www.imo.org/en/OurWork/Safety/Pages/ShipDesignAndStability-default.aspx>.

Orych, M., Werner, S. and Larsson, L. (2021) 'Validation of full-scale delivered power CFD simulations', *Ocean Engineering*, 238(July), pp. 1–10. doi: 10.1016/j.oceaneng.2021.109654.

Pizzigatti, C. and Franzoni, E. (2021) 'The problem of conservation of XX century architectural heritage: The fibreglass dome of the woodpecker dance club in Milano Marittima (Italy)', *Journal of Building Engineering*, 42(March 2021). doi: 10.1016/j.jobbe.2021.102476.

Poundra, G. A. P. et al. (2017) 'Optimizing trimaran yacht hull configuration based on resistance and seakeeping criteria', *Procedia Engineering*, 194, pp. 112–119. doi: 10.1016/j.proeng.2017.08.124.

Salehi-Khojin, A. et al. (2006) 'The role of temperature on impact properties of Kevlar/fiberglass composite laminates', *Composites Part B: Engineering*, 37(7–8), pp. 593–602. doi: 10.1016/j.compositesb.2006.03.009.

Sudjasta, B. and Djaya, Y. (2015) '10 GT Fishing Boat Design Made of Fiberglass for The Territorial Waters of Panimbang District Pandeglang Regency', *Bina Teknika*, 11(2), pp. 193–197. doi: 10.54378/bt.v11i2.112.

Sulistiyawati, W. and Suranto, P. J. (2009) 'Achieving Drag Reduction with Hullform Improvement in Different Optimizing Methods', *International Journal of Technology*, 45(3–4), pp. 1370–1379. doi: 10.14716/ijtech.11i7.4468.

Sulistiyawati, W., Yanuar and Pamitran, A. S. (2020) 'The influences of diversity hull shapes and outriggers arrangement in pentamaran systems', *Energy Reports*, 6, pp. 595–600. doi: 10.1016/j.egyr.2019.11.124.

Viljoen, H. C. et al. (2022) 'Effect of corrosion thinning on depth of operation: Case study of an HY-80 steel submarine pressure hull', *Marine Structures*, 81(October 2021), p. 103103. doi: 10.1016/j.marstruc.2021.103103.

Wolok, E. et al. (2017) 'Strength Analysis of Fiberglass Boat Hull Plates at Different Thickness', in, pp. 29–32.

Yang, L., Peng, Z. liang and Wang, D. yu (2018) 'Experimental and numerical investigation of material failure criterion with high-strength hull steel under biaxial stress', *Ocean Engineering*, 155(800), pp. 24–41. doi: 10.1016/j.oceaneng.2018.-02.022.